OPTICAL WAVEGUIDE TRANSITIONS

Most useful integrated optical waveguide devices use a series of waveguide transitions where the cross section of the waveguide structure changes in the direction of propagation. In the Mach Zehnder interferometer and in the directional coupler, both of which are commonly used, waveguide branches are used on both sides of a phase shift region to form an electrooptic modulator or switch. The performance of these devices depends on how well the transitions perform their intended function. To understand and optimize device performance it is therefore useful to be able to predict the transmission characteristics of waveguide transitions.

These characteristics are completely defined by Maxwell's equations. By using a computer approach, such as the beam propagation method (1,2), computer-generated solutions for each particular geometry of interest can be obtained. This approach has the advantage of providing accurate results for specific cases. However, computer approaches can be tedious and require multiple iterations to provide design guidance.

An alternative approach is the local normal mode formalism (3,4), an extremely powerful prediction tool. Coupling between local normal modes is caused by variations of waveguide parameters in the direction of propagation. With this formalism, the transmission properties of most waveguide transitions can be shown to depend on a few aggregate parameters which make most devices easy to understand and design. Under certain approximations, analytic solutions can be obtained to describe the amount of power transferred between these modes. These solutions can then be used to predict the performance of transition structures. The drawbacks of the local normal mode formalism include its inability to handle more than a limited number of modes (usually two), its inability to account for radiation, and its generally approximate representation.

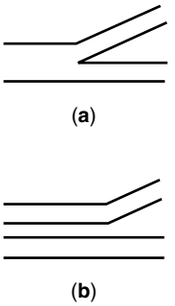

Figure 1. Waveguide branching structures. In (a) the waveguide branch is used to divide optical power or to separate normal modes. In (b) the separating waveguide is used to separate the outputs of two closely spaced channels.

In general the local normal mode formalism is useful for understanding the behavior of waveguide transitions and for giving approximate design information. Computer solutions are useful for more precise results, looking at the effects of radiation, and in cases where a two-mode formalism cannot be employed.

SEPARATING WAVEGUIDES AND HORNS

The most common waveguide transition structures are separating waveguides (also called branches) and horns. A separating waveguide may be a waveguide branch, as shown in Fig. 1(a), or the separating region of two closely coupled waveguides, as in Fig. 1(b). Waveguide branches are known as power dividers or mode splitters, depending on whether input power is divided between output arms of the branch, or whether the output power is predominately in a single output arm of the branch. Waveguide horns are used to change the dimensions of channel waveguides and to couple from planar guides to channel guides, as shown in Fig. 2. To provide a low loss transition, the horn must operate such that the input mode propagates through the structure without cumulative power transfer to higher order modes. Obviously any of these structures may be operated in reverse.

LOCAL NORMAL MODE FORMALISM

Normal Modes

For a simple three-layer waveguide structure a solution of Maxwell's equations for the guided modes of the structure

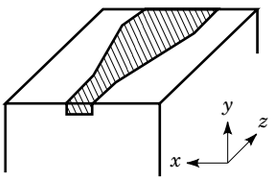

Figure 2. A channel waveguide horn is used as a transition structure to connect single-mode and multi-mode sections of waveguide.

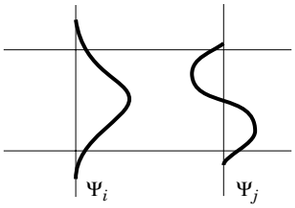

Figure 3. Electric field profiles for the first two normal modes of a three-layer waveguide. Normal modes are used in the modeling of transition structures.

yields electric-field profiles, shown in Fig. 3. These field solutions are called the normal modes of the waveguide. In Fig. 3 the geometry and optical wavelength are assumed such that the structure supports two normal modes. We will identify the first or symmetric mode as Ψ_i and the second or antisymmetric mode as Ψ_j. These modes have propagation constants β_i and β_j.

Local Normal Modes

By definition the normal modes of a structure are orthogonal, i.e., they satisfy the orthogonality condition

$$\int_{-\infty}^{\infty} \Psi_i(x)\Psi_j^*(x)\,dx = 0 \tag{1}$$

where x is the coordinate transverse to the waveguide. In waveguide transitions in which the waveguide layer thicknesses or indices vary in the direction of propagation (z), Eq. (1) is no longer true and one cannot strictly speak of the normal modes of the structure. Instead, we introduce the concept of a locally normal mode (5) as suggested in Fig. 4. At a waveguide position z_0, consider the waveguide parameters at that position, and solve for the normal modes of the structure as if it did not vary with z. These normal mode solutions are then said to be the local normal modes of the actual varying waveguide structure at the position z_0. The local normal mode representation will now become a function of z.

In contrast to the normal modes of a fixed structure, the amplitudes of the local normal modes in a varying waveguide structure are not necessarily constant. Power transfer occurs between the local normal modes of a varying structure, and the magnitude of that power transfer will depend on the rate

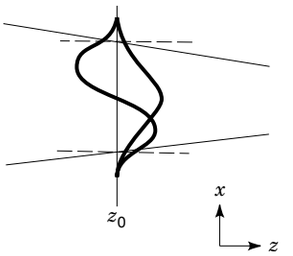

Figure 4. A local normal mode is defined by replacing the slowly varying waveguide structure at z_0 (solid line) with a structure constant with z (dashed line), and obtaining the normal mode solutions. Local normal modes are used as approximations to normal modes in transition structures.

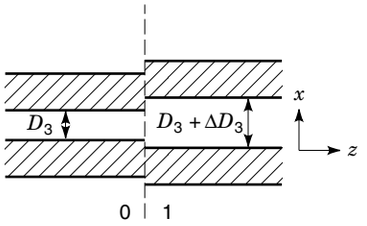

Figure 5. Abrupt transition at which the waveguide separation increases at a plane. This model represents a section of a branching or separating waveguide.

of change of the geometry of the structure. This rate of change can be either slow or fast, yielding adiabatic or abrupt transitions, respectively.

ADIABATIC AND ABRUPT TRANSITIONS

A slow or adiabatic waveguide transition is defined as a transition between two waveguide structures that takes place sufficiently gradually with propagation distance z so that negligible power transfer occurs between the local normal modes, as they propagate from one structure to the other. In an adiabatic transition, power injected in a given local normal mode will stay in that mode throughout the transition. The local normal mode may change its shape as the geometry changes, but coupling to other local normal modes is assumed not to occur.

The opposite extreme is a fast or abrupt transition in which a transition between two waveguide structures is made so abruptly that the maximum amount of power transfer between the local normal modes occurs, consistent with the geometry of the two waveguide structures. The limiting case of an abrupt transition is one that occurs at a plane, perpendicular to the direction of propagation of the modes. A plane or step transition is illustrated in Fig. 5. Power transfer between local normal modes at a step transition can be readily calculated from a consideration of boundary conditions at the transition.

COUPLED-MODE THEORY REPRESENTATION OF NORMAL MODES

For separating or branching waveguides, we will be dealing with two waveguides which can each independently support a single mode but which are sufficiently close to each other so that the optical fields of the two guides overlap in some region. The waveguides are then said to be coupled because transfer of optical power between them can occur. We first define the modes of the guides when they are uncoupled; that is, the separation between the guides approaches infinity so that optical coupling between them does not occur (Fig. 6). Then, if the waveguides are denoted a and b, the uncoupled mode field profiles are denoted by $\Phi_a = \Psi_{ia}$ and $\Phi_b = \Psi_{ib}$, and their propagation constants by β_a and β_b, respectively. These are the normal modes of each guide considered separately and are called the modes of the uncoupled waveguides.

Coupled-mode theory (6–8) is a perturbation approach which uses the modes of the uncoupled waveguides to describe optical power transfer between two coupled waveguides. It can also be used to provide an approximate representation for the normal modes of coupled waveguides (3,4).

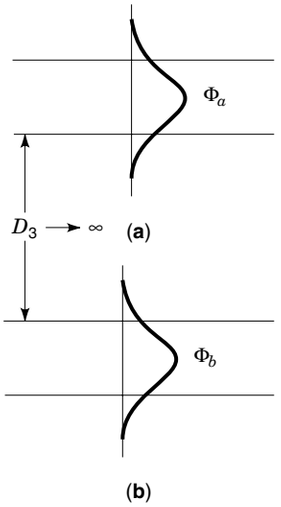

Figure 6. Uncoupled mode field profiles for waveguides at large separation. Linear combinations of these modes can be used to represent the normal modes of the coupled waveguides with finite D_3.

If D_3 is the separation between the two coupled waveguides of Fig. 7, the coupling coefficient between them is assumed to be of the form

$$K = K_0 e^{-\gamma_3 D_3} \tag{2}$$

where K_0 is a constant and γ_3 is the transverse component of momentum in the region between the waveguides. The difference in the guide propagation constants, at large separation, is $\Delta\beta = \beta_a - \beta_b$. We introduce the coupled waveguide parameter X:

$$X = \frac{\Delta\beta}{2K} \tag{3}$$

We show below that, in this approximation, power transfer between local normal modes at an abrupt transition between

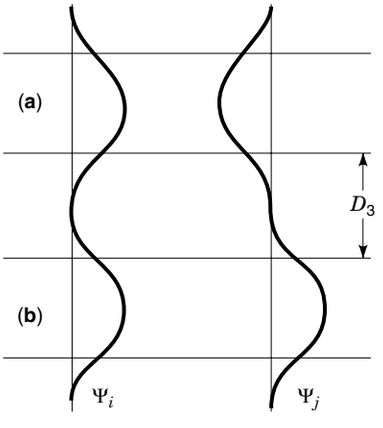

Figure 7. Coupled waveguides at finite separation. The coupled mode theory representation of the normal mode field profiles is shown for $\Delta\beta = 0$.

separating waveguides is a function only of the change in X across the transition.

For finite D_3 the normal modes of the coupled waveguide system of Fig. 7 can then be expressed as a linear combination of the uncoupled modes Φ_a and Φ_b

$$\Psi_i \approx d\Phi_a + e\Phi_b \tag{4a}$$

$$\Psi_j \approx -e\Phi_a + d\Phi_b \tag{4b}$$

Normalization is provided by $d^2 + e^2 = 1$. Since the normal modes should be orthogonal, Eq. (1) applies. However, this becomes an approximation due to the overlap of the uncoupled modes for finite D_3. The constants d and e are given by

$$d = \left\{\frac{1}{2}\left[1 + \frac{X}{(X^2+1)^{1/2}}\right]\right\}^{1/2} \tag{5a}$$

$$e = \left\{\frac{1}{2}\left[1 - \frac{X}{(X^2+1)^{1/2}}\right]\right\}^{1/2} \tag{5b}$$

The difference in normal mode propagation constant, $\Delta\beta_{ij} = \beta_i - \beta_j$, is

$$\Delta\beta_{ij} = 2K(X^2+1)^{1/2} \tag{6}$$

As an example of the coupled-mode theory representation of the normal modes, the case of $\Delta\beta = 0$ is plotted in Fig. 7. In this case $X = 0$, so $e = d$. The normal modes are made up of linear combinations of the uncoupled modes, with equal amplitude.

The coupled-mode theory representation of the normal modes outlined here is useful in that it provides an analytic representation with a direct dependence on the waveguide parameters. However, it is an approximation, and assumes either that the coupling is weak, or that the waveguides are not too dissimilar.

SCATTERING MATRIX FORMALISM

Four Port Model for a Waveguide Transition

In treating waveguide devices with arbitrary transitions it is useful to develop the scattering matrix for a generalized four-port junction (9). With this approach one can derive output equations for any device involving two normal modes. Consider a four port model of a general junction where modes i and j may enter or exit on sides 0 or 1. The waveguide transition may be any one or two guide structure, and may be adiabatic or abrupt, or intermediate between these two cases. The modes on a given side may coexist in the same waveguide, may be in separate waveguides, or a mode may have its power distributed between two waveguides. Back reflections, radiation, and losses are neglected, so that only forward scattering is accounted for. The scattering matrix $\boldsymbol{S}$ can be defined by (10):

$$\begin{bmatrix}\Psi_{i0}\\ \Psi_{j0}\\ \Psi_{i1}\\ \Psi_{j1}\end{bmatrix}_{\text{out}} = \begin{bmatrix}0 & 0 & S_{i0i1} & S_{i0j1}\\ 0 & 0 & S_{j0i1} & S_{j0j1}\\ S_{i1i0} & S_{i1j0} & 0 & 0\\ S_{j1i0} & S_{j1j0} & 0 & 0\end{bmatrix}\begin{bmatrix}\Psi_{i0}\\ \Psi_{j0}\\ \Psi_{i1}\\ \Psi_{j1}\end{bmatrix}_{\text{in}} \tag{7}$$

where the element S_{j1i0} denotes scattering from mode i incident on side 0 to mode j exiting from side 1, and so on. Equation (7) defines power division from a normalized input mode to the normalized output modes at a transition. For example, for mode i incident on side 0($\Psi_0 = \Psi_{i0}$), the output fields on side 1 are $S_{i1i0}\Psi_{i1}$ in mode i, and $S_{j1i0}\Psi_{j1}$ in mode j. The total output field is

$$\Psi_1 = S_{i1i0}\Psi_{i1} + S_{j1i0}\Psi_{j1} \tag{8}$$

Reciprocity and energy conservation require $\boldsymbol{S}$ to be symmetric and unitary (9). Then $S_{xy} = S_{yx}$ and the unique elements of Eq. (7) can be represented by

$$\begin{bmatrix}S_{i1i0} & S_{i1j0}\\ S_{j1i0} & S_{j1j0}\end{bmatrix} = \begin{bmatrix}(1-P)^{1/2}e^{j\phi_{i1i0}} & P^{1/2}e^{j\phi_{i1j0}}\\ P^{1/2}e^{j\phi_{j1i0}} & (1-P)^{1/2}e^{j\phi_{j1j0}}\end{bmatrix} \tag{9a}$$

with

$$\phi_{i1j0} + \phi_{j1i0} - \phi_{i1i0} - \phi_{j1j0} = \pm\pi \tag{9b}$$

where P is the power transferred between the local normal modes in the waveguide transition. Note that $P(j \rightarrow i) = P(i \rightarrow j)$. Equation (9b) provides the necessary relationship between the phases of the elements of the scattering matrix. These equations then totally define the scattering matrix for a general waveguide transition that supports two normal modes. For adiabatic transitions $P = 0$ and phases are immaterial. For abrupt transitions between separating waveguides we will see subsequently that power transfer and phases can be calculated analytically simply from a knowledge of the change in X at the transition. For intermediate transitions, between adiabatic and abrupt, power transfer and phases must be calculated numerically for each case.

Power Transfer at Abrupt Transitions

Next we show how the scattering matrix approach can be used to calculate P, the power transferred between local normal modes at an abrupt transition (10,11), for separating waveguides. Figure 5 shows a model abrupt transition, where two separating waveguides increase their separation by an amount ΔD_3 across the boundary. Propagation is assumed in the direction of increasing z and the regions before and after the boundary are denoted by 0 and 1. Since the local normal modes of a separating waveguide structure are characterized by the parameter X, the abrupt transition can be characterized in terms of the parameter X before (X_0) and after (X_1) the transition. An input mode i is assumed. The input mode $\Psi_0 = \Psi_{i0}$ is given by Eq. (4a), with d,e given by d_0,e_0. The output modes are given by Eqs. (4a) (for Ψ_{i1}) and (4b) (for Ψ_{j1}), with d,e given by d_1,e_1. The total output field is

$$\Psi_1 = (1-P)^{1/2}e^{j\phi_{i1i0}}\Psi_{i1} + P^{1/2}e^{j\phi_{j1i0}}\Psi_{j1} \tag{10}$$

For a plane boundary there is no accumulated phase across the boundary. We can pick three phases to be zero and the fourth must be chosen to satisfy Eq. (9b). This choice is related to the boundary conditions, and may be chosen consistent with the boundary conditions from a knowledge of

Table 1. Sign Rules for Mode Coupling at Abrupt Transitions

X increases	$i0 \rightarrow i1 + j1$
	$j0 \rightarrow j1 - i1$
X decreases	$i0 \rightarrow i1 - j1$
	$j0 \rightarrow j1 + i1$

whether X is increasing or decreasing across the boundary by using the sign rules given in Table 1.

The desired result is obtained by imposing the requirement of continuous transverse electric fields across the boundary, that is, $\Psi_0 = \Psi_1$. This yields

$$P = \frac{(f_1 - f_0)^2}{(f_1 - f_0)^2 + (1 + f_1 f_0)^2} \tag{11}$$

where $f_0 = e_0/d_0$ and $f_1 = e_1/d_1$, and $f(X)$ is given by

$$f = \frac{e}{d} = -X + (X^2 + 1)^{1/2} \tag{12}$$

For symmetric steps (about a centerline), Eq. (11) is independent of step size. For asymmetric steps, Eq. (11) is valid for small step sizes.

The approach developed in this section may be used to obtain the output equations for any device (12) composed of directional couplers, interferometric sections, and combining and separating branches, so long as the branches are assumed to be abrupt. It allows one to keep track of modal fields, and thus modal power, throughout the device, by serially treating each transition, phase shift, or coupling section. This formalism may be used to demonstrate how devices are affected when transitions assumed abrupt may in fact not be. For devices with transitions intermediate between adiabatic and abrupt this approach may still be used to develop output equations, but power transfer and mode phase changes in the intermediate transitions must be computed with a numerical technique.

COUPLED AMPLITUDE EQUATIONS

Single Step Model

One commonly used numerical approach to treat waveguide transitions is to divide the transition into a series of small abrupt steps, connected by regions of constant waveguide parameters, and calculate the mode propagation through this idealized geometry (13,14). For the single step of Fig. 5, the waveguide modes of interest are assumed to be incident on side 0, and the transmitted mode amplitudes are computed by imposing boundary conditions at the interface, i.e., the transverse field components must be continuous.

For two transverse electric (TE) guided modes, i and j, electric fields can be written as

$$E_y = a(z)\epsilon(x, z)e^{-j\alpha(z)} \tag{13a}$$

where

$$a(z) = \beta z + \phi \tag{13b}$$

Here $a(z)$ is the amplitude at a point z, $\epsilon(x,z)$ is the x-dependent field distribution, β is the mode propagation constant, and ϕ is a phase constant. Boundary conditions for TE modes require E_y and H_x to be continuous across the step. This requirement leads to a set of coupled amplitude equations given by

$$A_{j1}e^{-j\alpha_{j1}} = c_{ij}A_{i0}e^{-j\alpha_{i0}} + c_{jj}A_{j0}e^{-j\alpha_{j0}} \tag{14a}$$

$$A_{i1}e^{-j\alpha_{i1}} = c_{ii}A_{i0}e^{-j\alpha_{i0}} + c_{ji}A_{j0}e^{-j\alpha_{j0}} \tag{14b}$$

where

$$c_{ij} \approx \frac{I_{i0,j1}}{\sqrt{I_{i0,i0}I_{j1,j1}}} \tag{15}$$

and $I_{\gamma,\delta} = \int \epsilon_\gamma \epsilon_\delta dx$, for $\gamma,\delta = i,j$. In Eq. (14), A_γ is the mode amplitude a_γ normalized by a mode amplitude that corresponds to unity power. Values of c_{jj} and c_{ii} are obtained by the appropriate substitution of i and j in Eq. (15), and $c_{ji} = -c_{ij}$, a consequence of power conservation. These equations are appropriate for a single step. By dividing a transition into many small steps and iteratively applying these equations one can determine the output mode amplitudes, and thus powers, for the entire transition. The only requirement is that the fields throughout the structure are known. Later, we will show that approximate analytic expressions for c_{ij} can be obtained, so that specific knowledge of the fields can be avoided.

Differential Form

By transforming the coupled amplitude equations of Eq. (14) into differential equations we can obtain coupled mode equations for the local normal modes (15). These equations can be used to show that transitions shaped in a particular way have analytic solutions, within the approximations made. Alternatively they can be numerically solved themselves. The coupled amplitude equations can be expressed

$$A_{j1} = \sum_\gamma c_{\gamma i}A_{\gamma 0}, \qquad \gamma = i, j \tag{16a}$$

$$A_{i1} = \sum_\gamma c_{\gamma j}A_{\gamma 0}, \qquad \gamma = i, j \tag{16b}$$

which relate the transmitted local normal mode amplitudes on side 1 of a small step to those incident on side 0. The amplitudes are now considered to be complex so that $A_i = |A_i| \exp[-j(\beta_i z + \phi_i)]$. We generalize to a step in which an unspecified parameter p varies from p to $p + \delta p$ across the step. Thus, p may be the channel width in an expansion horn or the waveguide separation in a separating waveguide structure. We expect that c_{ij} will be proportional to the change δp across the step, and remove this dependence by defining a new coefficient C_{ij}

$$C_{ij} = \lim_{\delta p \rightarrow 0}\left(\frac{c_{ij}}{\delta p}\right) \tag{17}$$

For a small step $c_{jj} = c_{ii} \approx 1$, $c_{ij} = -c_{ji} = C_{ij}\delta p$, and Eq. (16) can be written as

$$\frac{dA_j}{dz} = C_{ij}\frac{dp}{dz}A_i - j\beta_j A_j \tag{18a}$$

$$\frac{dA_i}{dz} = -C_{ij}\frac{dp}{dz}A_j - j\beta_i A_i \tag{18b}$$

which are the differential equations describing coupling between the local normal modes. These equations will be referred to as the coupled normal mode equations.

Analytic Solutions

For specifically shaped transitions the coupled normal mode equations have an analytic solution (15,16). If $C_{ij}\ dp/dz = 0$, no power transfer between local normal modes occurs and the evolution of local normal mode i is described by a phase factor $\exp[-j\int_0^z \beta_i dz']$. Consider reduced mode amplitudes $a_i = A_i \exp[j\int_0^z \beta_i dz']$ and $a_j = A_j \exp[j\int_0^z \beta_j dz']$. The variation of p with z is determined by the shape of the transition. For a shape such that

$$\frac{dp}{dz} = \gamma\left(\frac{\Delta\beta_{ij}}{C_{ij}}\right) \tag{19}$$

where $\Delta\beta_{ij} = \beta_i - \beta_j$ and γ is an arbitrary constant, Eq. (18) becomes

$$\frac{da_j}{du} = \gamma e^{ju} a_i \tag{20a}$$

$$\frac{da_i}{du} = -\gamma e^{-ju} a_j \tag{20b}$$

where $u = \int_0^z \Delta\beta_{ij} dz'$. Equation (20) is a set of conventional coupled mode equations with constant coefficient γ for the amplitudes a_i and a_j. These equations have the solution for a_j

$$a_j = a_{i0}\frac{2\gamma}{\sqrt{(4\gamma^2+1)}} e^{ju/2}\sin\left[\frac{1}{2}(\sqrt{4\gamma^2+1})u\right] \tag{21}$$

for the initial conditions $a_i = a_{i0}$ and $a_j = 0$ at $z = 0$.

The quantity γ is a measure of the strength of the coupling between the local normal modes. For small γ the amount of power converted to mode j has a maximum value of

$$\frac{P_j^{\max}}{P_{i0}} = \frac{(a_j a_j^*)_{\max}}{a_{i0}a_{i0}^*} = \frac{4\gamma^2}{4\gamma^2+1} \tag{22}$$

Adiabatic structures should be designed with $\gamma \ll 1$, while abrupt structures need $\gamma > 1$. The approach considered here is valid if the principal coupling occurs between mode i and mode j, and coupling to other modes can be neglected.

Minimum Length Structures

Abrupt structures tend to be short and transition length is not a problem. However, adiabatic structures tend to be very long and it is of great practical interest to design minimum length structures. The shape described by Eq. (19) holds $(dp/dz)(C_{ij}/\Delta\beta_{ij})$ constant throughout the length of the transition. This results in a constant pressure or tendency for mode conversion between local normal modes everywhere (16,17). If we consider averages over mode interference effects, this should produce a transition which is as short as it can be for a given amount of allowed mode conversion.

COUPLED MODE THEORY REPRESENTATION OF C_{ij} AND $\Delta\beta_{ij}$

The coupled normal mode equations developed previously show that coupling between local normal modes in a transition structure is governed by the coupling coefficient between them, C_{ij}. Since we have analytic representations for the local normal modes from coupled mode theory, we can use these representations to calculate an analytic expression for C_{ij} (11,17). This is done here for the separating waveguide structure of Fig. 5, where the separation between guiding structures is increasing across the step. From Eqs. (15a) and (17) we have

$$c_{ij} = C_{ij}\Delta D_3 \approx \int_{-\infty}^{\infty} \Psi_{i0}\Psi_{j1}\, dx \tag{23}$$

where the parameter p is replaced by ΔD_3, the increase in separation between the two guiding regions across the step. Also, Ψ_{i0} refers to Ψ_i before the step on side 0, and Ψ_{j1} refers to Ψ_j after the step on side 1. Equation (23) is solved by substituting the coupled mode representation for the normal modes, yielding

$$C_{ij} = \frac{\gamma_3 X}{2(X^2+1)} \tag{24}$$

which gives C_{ij} as a function of X. This result is valid for symmetric branch shapes. For asymmetric separating waveguides, there will be a geometric contribution to C_{ij}, which is not included in Eq. (24). For separating waveguides, $\Delta\beta_{ij}$ is given by Eq. (6).

BRANCHES

The separating waveguide of Fig. 1(b) and the branching waveguide of Fig. 1(a) can be described in an equivalent manner if the parallel waveguides in Fig. 1(b) are sufficiently close for the normal modes to have power in both guiding regions. We will assume this to be true and from now on will refer generically to both structures as *branches.* Branches fall into two categories, depending on whether $\Delta\beta$ is or is not identically zero. For $\Delta\beta = 0$, it follows that $X = 0$ throughout the structure and no power transfer occurs. The normal mode shapes are defined by Eqs. (4) and (5) and each normal mode always has its power evenly divided between the two arms of the branch. Subsequently we will discuss the case $\Delta\beta \neq 0$, for linear and shaped branches.

Linear Branches

Linear branches have been treated both by coupled amplitude equations using the small step approximation (14) and by numerical integration of the coupled normal mode equations (18). As noted previously branch behavior can be separated into two classes, power dividers and mode splitters. Power dividers tend to divide input power between the output arms of the branch. In mode splitters output power is predominately in a single output arm of the branch, and the output arm selected depends on which input normal mode is excited. Power dividing and mode splitting behavior is illustrated in

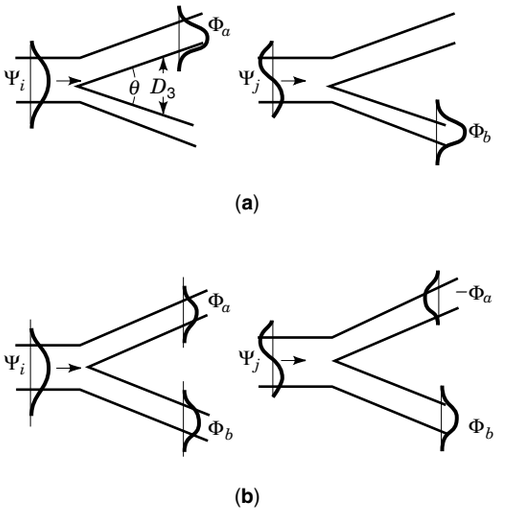

Figure 8. The limiting behavior of (a) mode splitting and (b) power dividing branches for single local normal mode input i or j. The mode splitting branch separates the local normal modes; the power dividing branch divides input optical power while maintaining relative phase between the branch arm outputs.

Fig. 8 for input normal modes i and j. By using the approximations of coupled mode theory, it has been shown (14) that operation as a mode splitter or as a power divider depends on whether

$$\frac{\Delta\beta}{\theta\gamma_3} > 0.43 \text{ or } \frac{\Delta\beta}{\theta\gamma_3} < 0.43 \tag{25}$$

Operation will be as a mode splitter if the first limit holds, and as a power divider if the second limit holds, where θ is the full branch angle. The validity of this dependence has been demonstrated for calculated branch output using the coupled amplitude equations (14), and by experimental branch results for $Ti:LiNbO_3$ channel waveguides (19).

This dependence on the quantity $\Delta\beta/\theta\gamma_3$ can also be demonstrated by transforming the coupled normal mode equations to a form appropriate for a linear branch (18). For a branch with separation D_3 between the arms, we have $\theta = dD_3/dz$, for small angles. The coupling coefficient K is given by Eq. (2), with $D_3 = 0$ at $z = 0$. Then, from Eq. (3), X can be expressed as $X = X_0 \exp[\gamma_3 D_3]$ where $X_0 = \Delta\beta/2K_0$ is the value of X at $z = 0$. The coupled normal mode equations [Eq. (18)] with $p \rightarrow D_3$, and with the reduced mode amplitudes introduced previously, can be written for constant θ as

$$\frac{da_j}{dX} = \frac{1}{2(X^2+1)} a_i \exp[-ju(X, X_0)] \tag{26a}$$

$$\frac{da_i}{dX} = -\frac{1}{2(X^2+1)} a_j \exp[ju(X, X_0)] \tag{26b}$$

where

$$u(X, X_0) = \frac{\Delta\beta}{\theta\gamma_3} \int_{X_0}^{X} \frac{\sqrt{X'^2+1}}{X'^2}\, dX' \tag{26c}$$

In Eq. (26) we have used coupled mode theory representations for $\Delta\beta_{ij}$ and C_{ij}. It is clear from this representation that branch behavior depends only on the parameter $\Delta\beta/\theta\gamma_3$ and the variation of $X(z)$ in the branch. This simple result is a consequence of constant θ in the linear branch. Eq. (26) can be integrated to obtain output mode amplitudes and phases.

Shaped Branches

As discussed previously the analytic solution to the coupled normal mode equations may be used to define a shaped branch with interesting properties (17). It has analytic solutions so that its behavior may be easily understood, and it can provide design guidance for minimum length structures. As assumed, we take $p \rightarrow D_3$ in Eqs. (18) and (19). Coupled mode theory approximations for $\Delta\beta_{ij}$ and C_{ij} are assumed. For branch angle θ (no longer a constant or necessarily small), Eq. (19) becomes

$$\tan\left(\frac{\theta}{2}\right) = \frac{1}{2}\frac{dD_3}{dz} = \gamma\frac{\Delta\beta}{\gamma_3}\frac{(X^2+1)^{3/2}}{X^2} \tag{27}$$

This result can be integrated to give the branch shape

$$\cos(\tan^{-1}X_0) - \cos(\tan^{-1}X) = 2\gamma\,\Delta\beta z \tag{28}$$

which is plotted in Fig. 9 for different values of X_0. In order to satisfy Eq. (27) with a constant γ, the branch angle θ becomes very large when the ratio $C_{ij}/\Delta\beta_{ij}$ is small, at the beginning and ends of the branch. In an actual device these large angles would have to be moderated to avoid excessive radiation losses. The minimum value of θ is

$$\theta_m = 3^{3/2}\frac{\gamma\,\Delta\beta}{\gamma_3} \tag{29}$$

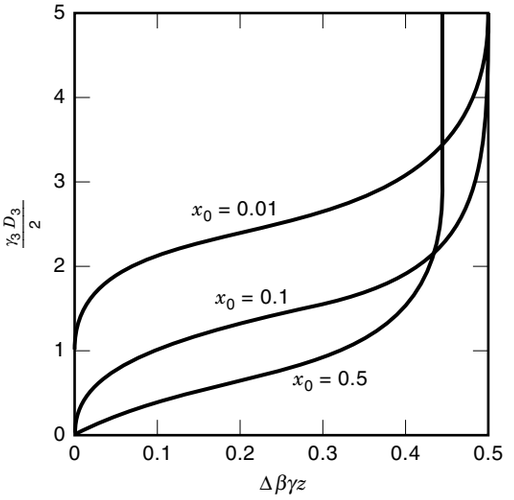

Figure 9. Normalized plot of branch arm separation versus direction of propagation z for shaped structures with initial conditions X_0. The shape is symmetric about a center line between the two guiding regions. This shaped structure maintains a constant level of power transfer between normal modes throughout its length.

which occurs at $X = \sqrt{2}$ where the coupling effects are the strongest ($C_{ij}/\Delta\beta_{ij}$ is a maximum). The branch length (l_b) is given by taking $D_3 \to 0$

$$l_b = \frac{1}{2\gamma\,\Delta\beta\sqrt{X_0^2 + 1}} \tag{30}$$

Adiabatic operation with smaller values of γ, therefore, corresponds to longer branches. Cumulative power conversion from mode i to mode j is given by Eq. (21)

$$\frac{|A_j|^2}{|A_{i0}|^2} = \frac{4\gamma^2}{4\gamma^2 + 1}\sin^2\left[\frac{u}{2}\sqrt{4\gamma^2 + 1}\right] \tag{31a}$$

with

$$u = \frac{1}{2\gamma}(\tan^{-1}X - \tan^{-1}X_0) \tag{31b}$$

which is a function of γ and X_0. This result allows one to calculate power transfer for a shaped branch. The interference term approaches $\approx 1/2$ for large values of γ and X, that is, at the branch output in the abrupt limit.

In the shaped structure defined previously, γ is a measure of the strength of the coupling between local normal modes and is held constant in the structure. In a linear branch, $\gamma \approx \theta C_{ij}/\Delta\beta_{ij}$ becomes z-dependent and a plot of γ versus z shows where mode coupling takes place in the branch. To demonstrate the length advantages of shaped structures we compare in Fig. 10 plots of γ versus z for comparable shaped and linear adiabatic branches. The linear branch has a constant θ equal to θ_m [obtained from Eq. (29)] for the shaped branch. The branches are chosen so that they produce comparable mode conversion. The length advantage for the shaped device is clear. However, as noted before, the shaped devices may have to be modified to maintain acceptable radiation loss, which may somewhat reduce their advantage.

Superposition of Solutions

For a single normal mode incident on a branch, its behavior can be understood in terms of the local normal modes of the structure, as in Fig. 8. For more complicated cases, with more than one mode incident, or with propagation reversed in the branch, outputs can be obtained by superposition of solutions

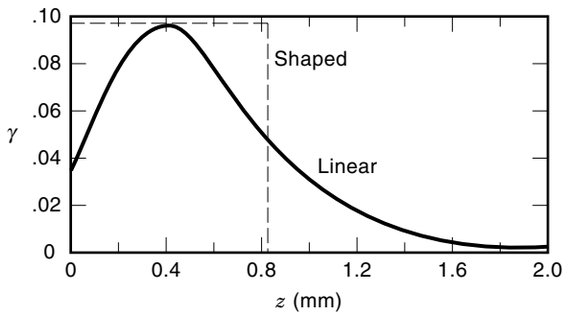

Figure 10. The parameter γ is plotted versus z for shaped and linear branches designed to be mode splitters. The magnitude of γ shows where power transfer between normal modes occurs in each branch.

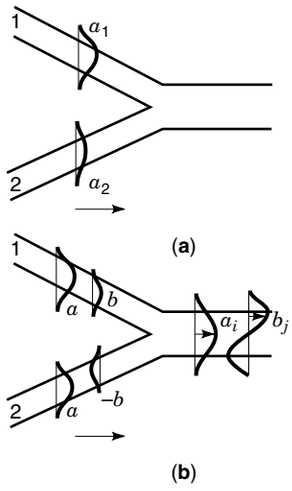

Figure 11. The use of superposition to solve a more complicated branching problem. In (a) unequal amplitudes a_1 and a_2 are incident on an ideal power dividing branch in reverse. In (b) the original modes are decomposed into a new set with in-phase amplitudes, a, and out-of-phase amplitudes, b, which combine to form output normal modes i and j.

already available (11). For example Fig. 11 shows the case of power incident on an ideal power dividing branch with $\Delta\beta = 0$, from the branch arms. We assume unequal powers incident with amplitude a_1 in guide 1 and a_2 in guide 2 ($a_1 > a_2$), but with equal phase [Fig. 11(a)]. We introduce a new set of mode amplitudes a and b defined by $a_1 = a + b$ and $a_2 = a - b$, and decompose the original set of modes into a new set with equal in-phase (a) and equal out-of-phase (b) amplitudes, as shown in Fig. 11(b). The in-phase mode amplitudes will combine to form local normal mode i in the output waveguide, and the out-of-phase mode amplitudes will combine to form local normal mode j. Conservation of power will show that the output amplitudes of modes i and j are related to the input amplitudes by $a_i = \sqrt{2}a$ and $b_j = b$. Problems of this kind can of course be worked out more formally using the scattering matrix approach developed earlier.

Current Branch Design

The overwhelming majority of branches and separating waveguides in current use in integrated optical devices are abrupt power dividers. Because these branches are so short (a few hundred microns in $Ti:LiNbO_3$), there is no incentive to use anything other than a linear branch. Adiabatic mode splitting branches are seldom used due to the long length required (5–10 mm in $Ti:LiNbO_3$) for good adiabatic operation. One important exception is the design of the active branching modulator (18,20) which is used in switch matrices (21,22) and in the *digital switch* (23). As shown in Fig. 12 the active branching modulator is a symmetric branch with electrodes placed to symmetrically raise and lower the index in opposing arms in a reversible, push–pull fashion. With no voltage applied, $\Delta\beta = 0$, and the device acts as a power divider. In one of its switch states a positive voltage is applied and the asymmetric index change makes $\Delta\beta$ large, so the device acts as an adiabatic mode splitter. By reversing the sign of the applied voltage, the asymmetric index change reverses, and power ex-

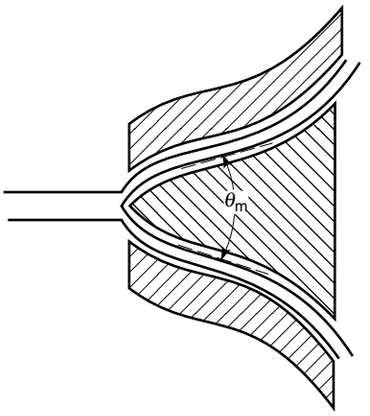

Figure 12. Active branching modulator with a shaped structure: θ_m is the minimum angle in the branch. A voltage is applied to the center electrode relative to the outside (grounded) electrodes, creating index changes of opposite polarity in the arms of the branch. The branch is driven to a mode splitter configuration, in which the input mode exits one output arm. Switching is achieved by changing the polarity of the applied voltage.

its the other arm, giving switching action. Minimizing the length of this adiabatic device has generated considerable theoretical and experimental (24) interest, with the shaped branch solution (25,26) playing a significant role.

WAVEGUIDE HORNS

Waveguide horns cannot make use of the coupled mode theory results for two coupled waveguides. However, the coupled normal mode equations do apply with $p \rightarrow W$, the waveguide width. In a horn we are generally interested in adiabatic propagation only, as typically one wants to expand the width of a channel waveguide while maintaining power in the lowest order mode. For symmetrical horns coupling between the first and second local normal modes does not occur (as the overlap integral is zero), and we will be concerned with coupling between the first and third order modes. First we give expressions for $\Delta\beta_{ij}$ and C_{ij} appropriate to this problem (16).

The value of $\Delta\beta_{ij}$ can be approximated from the dispersion relationship for a channel waveguide. The propagation constant difference for channel modes of different orders (first and third) in the x direction, but of the same order in the y direction (Fig. 2), is

$$\Delta\beta_{ij} = \frac{2\pi\lambda_g}{W^2} \tag{32}$$

where $\lambda_g = 2\pi/\beta_0$ is the modal wavelength in the guide for the first order mode. Also, C_{ij} can be obtained from a consideration of boundary conditions at a small step, and is given by

$$C_{ij} = -\frac{3}{4W} \tag{33}$$

for a step increasing with z. These results are valid in a wide channel where the modes are far from cut off. The ratio $|C_{ij}/\Delta\beta_{ij}|$ increases as W increases. This will result in an increasing coupling problem between the modes as W increases in a linear horn with constant θ. A solution to this problem is to shape the horn as described subsequently.

For an analytic solution to the coupled normal mode equations using a shaped horn (16), the required horn shape is obtained by substituting $p \rightarrow W$ in Eq. (19). Using the expressions obtained for $\Delta\beta_{ij}$ and C_{ij} in that result yields the local horn angle θ (Fig. 13)

$$\theta \equiv \frac{1}{2}\frac{dW}{dz} = -\gamma\frac{4\pi}{3}\frac{\lambda_g}{W} \tag{34}$$

where γ is a constant. The shape of this horn will be parabolic with

$$W = (2\alpha\lambda_g z + W_0^2)^{1/2} \tag{35}$$

where W_0 is the horn width at $z = 0$ and $\alpha = -8\pi\gamma/3$. The solution of power transfer from initial mode i to mode j is given by Eq. (31a), with u given by $(2\pi/\alpha)\ln(W/W_0)$.

Arguments for the length efficiency of this shape are the same as those made earlier for the shaped branch. With a parabolic shape $\gamma = 2C_{ij}\theta/\Delta\beta_{ij}$ remains constant throughout the horn, and the strength of mode coupling between i and j is evenly distributed along the length. This is not true for other horn shapes where γ will be a function of z. For the same amount of mode conversion, in horns with the same expansion, the parabolic horn should be shorter than other shapes, within the approximations made.

DIRECT COMPUTATIONAL METHODS

An alternative to the coupled mode theory approach is a direct computational approach which calculates the propagation of light through a waveguide structure by applying an appropriate computational scheme to the wave equation. One only needs to assume the geometry of the index distribution, which may vary with z, the input field, and any approximations inherent in the computational scheme employed. Entire devices including a variety of transition structures can be calculated, given sufficient computer resources. Although a number of suitable computation schemes exist, only the more commonly used beam propagation method (BPM) (1,2) will be discussed here. The BPM is a split operator method used to solve the scalar homogeneous Helmholtz equation. It effec-

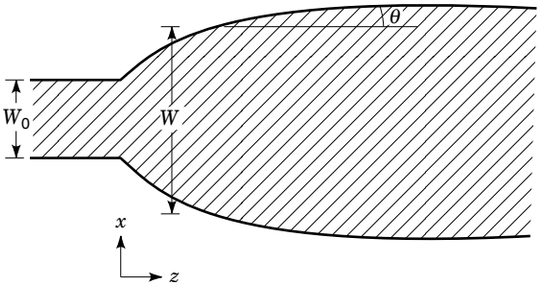

Figure 13. Parabolic channel waveguide horn. Using the parabolic geometry allows one to analytically calculate horn transmission.

tively models an optical structure as a series of infinitely thin lenses separated by an incremental axial distance Δz.

For monochromatic light propagating in an optical waveguide, the homogeneous Helmholtz equation is (27)

$$\nabla^2 \overline{E} = \frac{\omega^2}{c^2} n^2(x, y)\overline{E} = 0 \tag{36}$$

where the refractive index $n(x,y)$ is assumed to depend only on the x and y coordinates. For a forward propagating field in the $+z$ direction, $\overline{E}(\omega,x,y,z)$ may be expressed as $E(x,y)\exp(-jkz)$, where $k = n_0\omega/c$, and n_0 is the index of the substrate. With these assumptions one can obtain

$$\frac{\partial}{\partial z}E' + \frac{j}{2}\left[\nabla_\perp^2 + k^2\left(\frac{n^2}{n_0^2} - 1\right)\right]E' = 0 \tag{37a}$$

where

$$\nabla_\perp^2 = \frac{\partial^2}{\partial x^2} + \frac{\partial^2}{\partial y^2} \tag{37b}$$

This is the paraxial or Fresnel form of the wave equation where E' denotes a slowly varying approximation for the field in the z direction. This form has a solution which we write as (28)

$$E'(x, y, \Delta z) = \exp\left(-\frac{j\Delta z}{2k}\nabla_\perp^2\right) \exp\left[-\frac{j\Delta z}{2k}k^2\left(\frac{n^2}{n_0^2} - 1\right)\right]E'(x, y, 0) \tag{38}$$

where $E'(x,y,0)$ is the initial condition of the field at $z = 0$. Equation (38) is written with two exponential factors which is the basis for the BPM. The two factors represent a step of propagation over a length Δz, and a phase or lens term. This approach provides a method of visualizing the propagation process by replacing the waveguide with a series of infinitely thin lenses, separated by the axial distance Δz. By using a Fourier series representation of the initial field, one can use fast Fourier transform algorithms to implement the propagation terms in Eq. (38). This allows for algebraic implementation of the propagation term in the spatial frequency domain, while the phase or lens term is performed with simple multiplication in the spatial domain. The BPM then consists of a set of Fourier transforms interspersed with complex multiplications in the spatial domain in an iterative algorithm, thus advancing the solution in successive steps along the optic axis (29). The BPM approach has been widely used for a variety of transition structures.

BIBLIOGRAPHY

1. J. van Roey, J. van der Donk, and P. E. Lagasse, Beam-propagation method: Analysis and assessment, *J. Opt. Soc. Am.,* **71**: 803-810, 1981.
2. L. Thylen, The beam propagation method: An analysis of its applicability, *Opt. Quantum Electron.,* **15**: 433-439, 1983.
3. A. G. Fox, Wave coupling by warped normal modes, *Bell Syst. Tech. J.,* **34**: 823-852, 1955.
4. W. H. Louisell, Analysis of the single tapered mode coupler, *Bell Syst. Tech. J.,* **34**: 853-870, 1955.
5. D. Marcuse, *Theory of Dielectric Optical Waveguides,* New York: Academic, 1974, Chapt. 3.
6. S. E. Miller, Coupled wave theory and waveguide applications, *Bell Syst. Tech. J.,* **33**: 661-719, 1954.
7. W. H. Louisell, *Coupled Mode and Parametric Electronics,* New York: Wiley, 1960.
8. A. Yariv, Coupled-mode theory for guided wave optics, *IEEE J. Quantum Electron.,* **QE-9**: 919-933, 1973.
9. D. S. Jones, *The Theory of Electromagnetism,* New York: Macmillan, 1964, pp. 254-261.
10. W. K. Burns, Normal mode analysis of waveguide devices. Part I: Theory, *J. Lightwave Tech.* **6**: 1051-1057, 1988.
11. W. K. Burns and A. F. Milton, Waveguide transitions and junctions, in T. Tamir (ed.), *Guided-Wave Optoelectronics,* Berlin: Springer-Verlag, 1988.
12. W. K. Burns, Normal mode analysis of waveguide devices. Part II: Device output and crosstalk, *J. Lightwave Tech.* **6**: 1058–1068, 1988. (see also errata, *J. Lightwave Tech.* **7**: 1425, 1989.)
13. D. Marcuse, Radiation losses of tapered dielectric slab waveguides, *Bell Syst. Tech. J.,* **49**: 273-290, 1970.
14. W. K. Burns and A. F. Milton, Mode conversion in planar-dielectric separating waveguides, *IEEE J. Quantum Electron.,* **QE-11**: 32-39, 1975.
15. A. F. Milton and W. K. Burns, Mode coupling in tapered optical waveguide structures and electrooptic switches, *IEEE Trans. Circuits Syst.,* **CAS-26**: 1020-1028, 1979.
16. A. F. Milton and W. K. Burns, Mode coupling in optical waveguide horns, *IEEE J. Quantum Electron.,* **QE-13**: 828-835, 1977.
17. W. K. Burns and A. F. Milton, An analytic solution for mode coupling in optical waveguide branches, *IEEE J. Quantum Electron.,* **QE-16**: 446-454, 1980.
18. W. K. Burns, M. M. Howerton, and R. P. Moeller, Performance and modeling of proton exchanged $LiTaO_3$ branching modulators, *J. Lightwave Tech.,* **10**: 1404-1408, 1992.
19. W. K. Burns et al., Optical waveguide channel branches in Ti-diffused $LiNbO_3$, *Appl. Opt.,* **19**: 2890-2896, 1980.
20. W. K. Burns, A. B. Lee, and A. F. Milton, Active branching waveguide modulator, *Appl. Phys. Lett.,* **29**: 790, 1976.
21. P. Granestrand et al., Integrated optics 4x4 switch matrix with digital optic switches, *Electron. Lett.,* **26**: 4, 1990.
22. A. C. O'Donnell, Polarization independent 1×16 and 1×32 lithium niobate optical switch matrices, *Electron. Lett.,* **27**: 2349, 1991.
23. Y. Silberberg, P. Perlmutter, and J. E. Baran, Digital optical switch, *Appl. Phys. Lett.,* **51**: 1230, 1987.
24. H. Okayama, T. Ushikubo, and M. Kawahara, Low drive voltage Y-branch digital optical switch, *Electron. Lett.,* **27**: 24, 1991.
25. W. K. Burns, Voltage-length product for modal evolution-type digital switches. *J. Lightwave Tech.,* **8**: 990-997, 1990.
26. W. K. Burns, Shaping the digital switch, *IEEE Photon. Tech. Lett.,* **4**: 861-863, 1992.
27. M. D. Feit and J. A. Fleck, Jr., Mode properties and dispersion for two optical fiber-index profiles by the propagating beam method, *Appl. Optics,* **19**: 3140-3150, 1980.
28. M. D. Feit and J. A. Fleck, Jr., Light propagation in graded-index optical fibers, *Appl. Optics,* **17**: 3990-3999, 1978.
29. P. E. Pace and C. C. Foster, Beam propagation analysis of a parallel configuration of Mach-Zehnder interferometers, *Optical Engr.,* **33**: 2911-2921, 1994.

W. K. BURNS
Naval Research Laboratory

OPTICS, MATERIALS. See OPTICAL MATERIALS.
OPTICS, NONLINEAR. See NONLINEAR OPTICS.